The Astrophysical Journal, 513:L5–L8, 1999 March 1

SHORT-TIMESCALE VARIABILITY IN THE EXTERNAL SHOCK MODEL OF GAMMA-RAY BURSTS

Charles D. Dermer[1] and Kurt E. Mitman[1,2]

Received 1998 September 25; accepted 1999 January 6; published 1999 January 28

ABSTRACT

We have developed a computer model to calculate gamma-ray burst (GRB) light curves and efficiencies from the interaction of a single, thin blast wave with clouds in the external medium. Large-amplitude, short-timescale variability occurs when the clouds have radii $r \ll R/\Gamma$, where R is the mean distance of a cloud from the GRB source and Γ is the blast-wave Lorentz factor. Efficiencies $\gtrsim 10\%$ require a large number of small clouds, each with sufficiently large column densities to extract most of the available blast-wave energy in the region of interaction. The number and duration of pulses in the simulated GRB light curves are compared with the respective properties found in GRB light curves. If GRB sources are surrounded by clouds with such properties, then short-timescale variability of GRBs can be obtained in the external shock model.

Subject headings: gamma rays: bursts — radiation mechanisms: nonthermal

1. INTRODUCTION

The cosmological origin of gamma-ray bursts (GRBs) has been established as a result of optical follow-up observations of fading X-ray counterparts to GRBs that were discovered with the *BeppoSax* mission (see, e.g., Costa et al. 1997; van Paradijs et al. 1997; Djorgovski et al. 1997). The total energy released in GRB 970508 and GRB 971214 exceeds 10^{52} ergs (see, e.g., Waxman 1997) and 10^{53} ergs (Kulkarni et al. 1998), respectively, if the emission is unbeamed. The time profiles of the X-ray afterglow light curves are generally well fitted by power laws (see, e.g., Piro et al. 1998 and Feroci et al. 1998).

These observations provide support for the fireball/blast-wave model of GRBs (Rees & Mészáros 1992). In this model, a large quantity of energy that is released in a small volume produces a GRB when the baryon loading of the fireball yields a blast wave with a Lorentz factor of $\Gamma \sim 100$–300. Such values of Γ are required in order to avoid significant attenuation of gamma rays through pair production processes (see, e.g., Baring & Harding 1997). Fireballs with larger and smaller baryon loading are difficult to detect because of design limitations of past telescopes (Dermer, Chiang, & Böttcher 1999).

The success of the relativistic blast-wave model is due largely to the relative simplicity with which it explains the temporal dependence and intensity of the long-wavelength GRB afterglows (see, e.g., Wijers, Rees, & Mészáros 1997; Waxman 1997; Vietri 1997; Chiang & Dermer 1999). Power-law decays in the afterglow light curves result from the deceleration of the blast wave as it becomes energized by sweeping up material from the circumburst medium (CBM). This is termed the external shock model of GRBs and was originally introduced to provide a mechanism for converting the energy of the blast wave into radiation during the prompt gamma-ray–luminous phase of GRBs (Mészáros & Rees 1993).

Recent research (Fenimore, Madras, & Nayakshin 1996; Sari & Piran 1997; Fenimore et al. 1999) indicates that the external shock model faces difficulties in explaining short-timescale variability (STV) in GRB light curves and afterglows as a consequence of special relativistic effects resulting from the curvature of the blast wave shell. In this Letter, we construct a computer model in order to examine the requirements of an external shock model to produce STV. In § 2, we outline the temporal spreading problem due to the curvature of a blast wave. Our numerical model used to simulate this system is described in § 3, and results are presented in § 4. If STV in GRB light curves is due to an external shock model, then the required characteristics of such a model are outlined in § 5.

2. VARIABILITY FROM LOCALIZED BLAST-WAVE EMISSION REGIONS

The STV problem in the external shock model is illustrated in Figure 1. A blast wave, expanding with Lorentz factor Γ, sweeps up material from a density inhomogeneity, or "cloud," located at a distance R from the explosion site. We assume for simplicity that the cloud is spherical with radius r. Let θ represent the angle between the directions from the GRB explosion site to an observer and to the center of the cloud. The blast wave first interacts with the cloud at point 1 and stops interacting when it reaches point 4. The largest angular extent of the blast wave energized by the cloud is defined by the locations of points 2 and 3. The observer will record photon arrival times from each of the four points. The time delay between photons emitted from points 1 and 4 is

$$\Delta t_r = \frac{2r}{\beta c}(1 - \beta \cos\theta)(1 + z) \equiv \frac{2r(1 + z)}{\beta c \Gamma \mathcal{D}} \cong t_{\rm dur}\left[\frac{r}{R}(1 + \theta^2\Gamma^2)\right], \quad (1)$$

where the Doppler factor $\mathcal{D} = [\Gamma(1 - \beta\cos\theta)]^{-1}$, $\beta = (1 - 1/\Gamma^2)^{1/2}$, and z is the redshift. The quantity $t_{\rm dur} \equiv R_{\rm max}(1 + z)/(\Gamma^2 c)$ represents the characteristic duration of emission observed from a blast wave that radiates as it passes through a medium of maximum extent $R_{\rm max} > R$. The expression on the right side of equation (1) holds in the limit $\Gamma \gg 1$, implying that $\theta \ll 1$ because most of the radiation is observed from a cone of angular extent $\lesssim 1/\Gamma$ owing to the Doppler effect. For constant Γ, the time delay between photons emitted from points

[1] E. O. Hulburt Center for Space Research, Code 7653, US Naval Research Laboratory, Washington, DC 20375-5352.

[2] Thomas Jefferson High School for Science and Technology, 6560 Braddock Road, Alexandria, VA 22312.

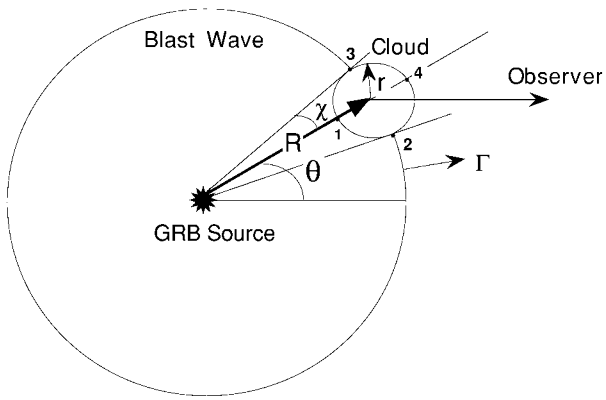

FIG. 1.—Geometry of the interaction between a blast wave and a cloud in the CBM.

2 and 3 is

$$\Delta t_a = \frac{2R}{c} \sin\theta \sin\chi (1+z) \cong t_{\rm dur} \left[\frac{r}{R} (2\Gamma^2 \theta) \right] , \qquad (2)$$

where we assume that $r/R \ll 1$ and $\Gamma \gg 1$ in the rightmost expression of equation (2).

The term Δt_r is a radial spreading timescale that is related to the observed interval over which the blast wave passes through the radial extent of the cloud, and the term Δt_a is an angular spreading timescale that is related to the angular extent of the cloud (see Fenimore et al. 1996 and Sari & Piran 1997). The shortest temporal duration from the blast-wave/cloud interaction is defined by the maximum of these two timescales. Note, however, that the pulse width from an interaction event could be longer then the kinematic minimum timescale derived here if the blast wave does not decelerate or radiate its swept-up energy rapidly, or if the blast-wave shell has thickness $l \gtrsim r$. In the limit that the blast wave is approximated by expanding collisionless particles, $l \sim R/(2\Gamma^2)$ (Mészáros, Laguna, & Rees 1993). The shell would be much thinner, however, if treated as a radiative hydrodynamical fluid that is compressed by the pressure of the external medium (Blandford & McKee 1976), and we assume that this is the case here.

As can be seen by comparing equations (1) and (2), Δt_a is much longer than Δt_r, except within a very narrow cone of extent $\theta \lesssim 1/(2\Gamma^2)$. If the blast wave is uncollimated, much of the observed radiation is produced from interactions near $\theta \sim 1/\Gamma$ where $\Delta t_a/\Delta t_r \sim \Gamma$. Therefore, to produce STV with $\Delta t_a < \delta t \ll t_{\rm dur}$ requires very small clouds with $r/(R/\Gamma) \lesssim (\delta t/t_{\rm dur})$. GRB time profiles commonly show pulses with $\delta t/t_{\rm dur} \lesssim 0.01$–$0.1$; thus, very small clouds that, individually, have a small surface covering factor are required for STV. The average covering factor is the ratio of the total area of the clouds to the area of the beaming cone and is given by $\approx I_c \pi r^2/[\pi(R_{\rm max}/\Gamma)^2] \equiv I_c f^2$, where I_c is the number of clouds in the beaming cone and $f \equiv r/(R_{\rm max}/\Gamma)$. The efficiency for extracting energy from a blast wave is therefore roughly equal to

$$\zeta = \min(N_c/N_{\rm cd}, 1) I_c f^2 . \qquad (3)$$

Here N_c is the column density of a cloud, and $N_{\rm cd}$ is the column density that a cloud must have in order to extract a significant fraction of the available energy in the portion of the blast wave that interacts with the cloud. Here we implicitly assume that a large fraction of the blast-wave energy is converted to nonthermal electrons and then to radiation. If this is not the case, then the efficiency is reduced and the energy requirements increased accordingly. If the explosion energy $E_0 = 10^{54} E_{54}$ ergs is emitted uniformly in all directions from the explosion site, then strong deceleration occurs when the swept-up relativistic cloud mass Γm_c equals the baryonic mass in the region that interacts with the cloud, where $m_c = 4\pi N_c m_p r^2/3$ is the cloud mass. This implies $N_{\rm cd} \cong 3E_0/(16\pi\Gamma^2 m_p c^2 R^2) = 4.4 \times 10^{16} E_{54}/\Gamma_{300}^2 R_{17}^2$ cm^{-2}, where $\Gamma = 300\Gamma_{300}$ and $R = 10^{17} R_{17}$ cm.

In order to extract the blast wave's energy efficiently by interacting with clouds, we see from equation (3) that a large number of clouds with thick columns (i.e., $N_c \gtrsim N_{\rm cd}$) are required to offset their small size. If, for example, $f = 0.01$, then $\gtrsim$1000 clouds with thick columns within the Doppler beaming cone will give an efficiency $\zeta \gtrsim 0.1$. It has been argued that pulses from the individual clouds would overlap (Sari & Piran 1997; Sumner & Fenimore 1998) and fail to produce light curves with large-amplitude variability when the efficiencies are large. We have constructed a model to assess this claim quantitatively.

3. DESCRIPTION OF THE MODEL

We use Monte Carlo methods to simulate the interaction of a spherically expanding blast wave with clouds in the CBM. The clouds are randomly distributed in angle, azimuth, and location. The radial distribution can be generally chosen, but for purposes of illustration, we consider a uniform distribution in the range $R < R_{\rm max} = 10^{17}$ cm. The mass and radius distributions of clouds can also be generally chosen, but here we consider for clarity the case where all clouds have equal radii. In the results shown here, we assume that the clouds have thick columns. This means that $N_c \gtrsim 4 \times 10^{18}$ cm^{-2} for clouds with $R > 10^{16}$ cm; closer clouds require larger column densities, but the number of such clouds is extremely small. We employ a blocking factor to account for occulted clouds. After the locations and radii of the clouds are selected, the program determines which clouds have been completely occulted and eliminates them. When partial occultation occurs, we weight the contribution of that cloud based on the fraction of the area that is occulted.

We use the following expression to represent the angle-dependent flux density S (ergs cm^{-2} s^{-1} $\epsilon_{\rm obs}^{-1}$) measured at observer time $t_{\rm obs}$ from that portion of the curved blast-wave surface that is energized by its interaction with a cloud:

$$S(\epsilon_{\rm obs}, t_{\rm obs}; \Omega_{\rm obs}) = K \frac{\mathcal{D}^3 (1+z) J(\epsilon)}{4\pi d_L^2} 4 \left(\frac{\ln 2}{\pi} \right)^{1/2} e^{-(t_c - t_{\rm obs})^2/2\sigma^2} , \qquad (4)$$

where

$$K = 1 \text{ and } \Delta t = \Delta t_r, \text{ if } \theta \leq 1/(2\Gamma^2)$$

$$K = r(R\Gamma\mathcal{D} \sin\theta \sin\chi)^{-1} \cong (\Gamma\theta\mathcal{D})^{-1} \text{ and } \Delta t = \Delta t_a, \quad \text{if } \theta > 1/(2\Gamma^2) \qquad (5)$$

(see Dermer, Sturner, & Schlickeiser 1997). In equation (4), we approximate the pulse duration by a Gaussian function with $\sigma = \Delta t/[4(2\ln 2)^{1/2}]$, which gives an FWHM pulse duration equal to $\Delta t/2$. In equation (5), $\epsilon_{\rm obs} = h\nu_{\rm obs}/m_e c^2 = \mathcal{D}\epsilon/(1+z)$ is the observed dimensionless photon energy, and ϵ is the photon energy measured in the comoving frame of the blast wave, $t_c = (1+z)R(1-\beta\cos\theta)/(\beta c)$ when $\Delta t_r > \Delta t_a$ and $t_c = (1+z)R(1-\beta\cos\theta\cos\chi)/(\beta c)$ when $\Delta t_r < \Delta t_a$. The quantity $J(\epsilon)$ represents the spectral power in the comoving frame. The above result is obtained by noting that in the limit $r \ll R/\Gamma$, the beaming factor for the time-integrated fluence from the radiating portion of the blast wave energized by the interaction is the same as that for a spherical ball of plasma that radiates for a comoving period of time equal to $t_2 - t_1 = 2r/\beta\Gamma c$.

We approximate the comoving radiant emission by a power law such that $J(\epsilon) = J_0\epsilon^{-\alpha}$ in the energy range $\epsilon_1 \le \epsilon \le \epsilon_2$, where α is the photon energy index. To set the normalization for J_0, we note that due to the increasing surface area of the expanding blast wave, the maximum energy that could be radiated as a result of the blast-wave/cloud interaction is just $E_c \cong [E_0 r^2/(4R^2)]\min(N_c/N_{\rm cd}, 1)$. We assume that this energy is radiated promptly; that is, the interaction takes place in the radiative regime. The relationship between the measured energy fluence F_E (ergs cm^{-2}) and the total energy emitted is $F_E = (1+z)E_c/(4\pi d_L^2)$, where d_L is the luminosity distance. From this relation, we obtain the result $J_0 = f_\alpha[E_c/\Gamma(t_2 - t_1)] = f_\alpha(cE_c/2r)$, where $f_\alpha \equiv (1-\alpha)/(\epsilon_2^{1-\alpha} - \epsilon_1^{1-\alpha})$.

4. RESULTS

In our calculations, we choose parameter values motivated by the observations of the candidate host galaxy of GRB 971214 at redshift $z = 3.42$ (Kulkarni et al. 1998). Its total energy release, including prompt radiation and afterglow, could exceed 10^{54} ergs if the burst source is unbeamed. Thus, we choose a value of $\partial E/\partial\Omega = 10^{53}$ ergs sr^{-1} for our standard GRB energy release, which implies a value of $E_{54} = 1.3$ if the burst energy is isotropically radiated. For the calculations shown here, we let $\Gamma_{300} = 1$, $z = 1$ (which implies $d_L = 1.67 \times 10^{28}$ cm for a Hubble constant of 65 km s^{-1} Mpc^{-1} and $q_0 = \frac{1}{2}$), $\alpha = 1$, $\epsilon_1 = 10^{-4}$, and $\epsilon_2 = 10^2$. In order to conserve computing time, all clouds are placed at angles $\theta < k_\theta/\Gamma$ with $k_\theta = 3$, since we find that clouds located at larger angles make a negligible contribution to the observed flux because of the strong Doppler beaming. The clouds are located in a shell between $R_{\rm min} = 10^{16}$ and $R_{\rm max} = 10^{17}$ cm.

Figure 2 shows results of our calculations for a range of different cloud sizes at $\epsilon_{\rm obs} = 1$. The number of clouds within the Doppler beaming cone $\theta < 1/\Gamma$ is chosen in order to obtain a 10% efficiency as defined by equation (3). In curves (a), (b), and (c), we let $f = r/(R_{\rm max}/\Gamma) = 0.1$, 0.03, and 0.01, implying a total number of clouds $k_\theta^2 I_c = 9I_c = 90$, 1000, and 9000 in the respective calculations. From the expression for $N_{\rm cd}$ following equation (3), this implies cloud densities $n_c \gtrsim 100E_{54}/(\Gamma_{300}R_{17}^3 f)$ cm^{-3}. By examining the curves, one can verify that the calculated energy fluences agree with the expected energy fluence $\cong 0.1(1+z)4\pi \times 10^{53}$ ergs sr$^{-1}/[4\pi d_L^2\ln(\epsilon_2/\epsilon_1)] \sim 5 \times 10^{-6}$ ergs cm^{-2} for a 10% efficiency.

From equation (2), we see that a typical pulse duration is $\approx\Delta t_a \approx 2r(1+z)/(\Gamma c)$ when $\theta \sim 1/\Gamma$. The cloud size in curve (a) has a value of $r = 3.3 \times 10^{13}$ cm, implying $\delta t = 15$ s when $\theta \sim 1/\Gamma$, comparable to the value of $t_{\rm dur} = 74$ s. Thus, only limited structure in the light curves is seen. For the cases with smaller clouds shown in curves (b) and (c), the light curves become increasingly variable. In some cases, a very narrow pulse with large amplitude is obtained as a result of a cloud that happens to be located within an angle $\theta \lesssim 1/\Gamma^2$ of the observer's line of sight. The light curves are most variable during the period $\approx(1+z)(R_{\rm max} - R_{\rm min})/(2\Gamma^2 c) \sim 33$ s. The tendency for longer pulses to be found in the simulated light curves at later times is an artifact of the bounded cloud ranges in the numerical simulation. This effect is ameliorated when more complicated cloud profiles without sharp boundaries are considered. All these simulated GRBs would be detectable with BATSE on the *Compton Gamma Ray Observatory* (*CGRO*) out to redshifts $z \approx 4$, noting that BATSE triggers on a νF_ν flux of $\gtrsim 10^{-7}$ ergs cm^{-2} s^{-1}. Higher efficiency events could be detected from sources at even larger redshifts (see inset to Fig. 2).

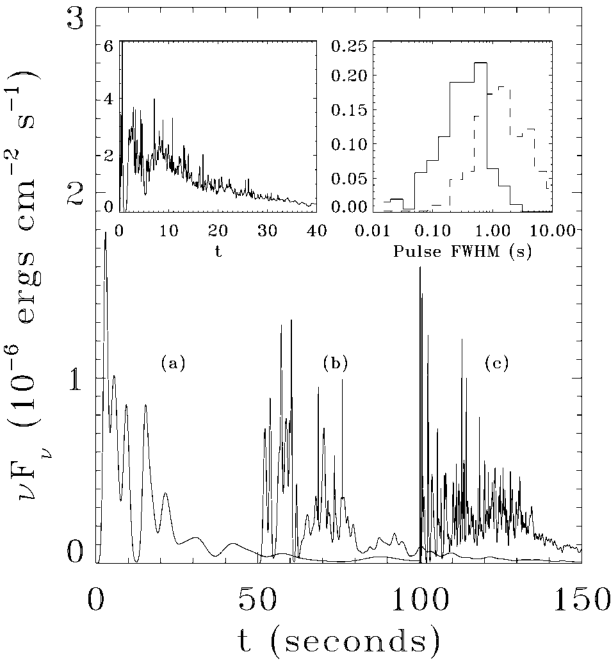

FIG. 2.—Simulated light curves from blast-wave/cloud interactions. The cloud radii range from 3.3×10^{13} cm in curve (a) to 3.3×10^{12} cm in curve (c), and the total number of clouds is estimated from eq. (3) in order to extract 10% of the blast-wave energy (see text). Successive curves are offset by 50 s each for clarity. The left inset shows a calculation for 3.3×10^{12} cm clouds giving ~100% efficiency. The right inset shows the distributions of pulse widths, normalized to unity, for an ensemble of light curves with cloud sizes corresponding to curves (b) and (c), which are represented by the solid and dashed histograms, respectively. The early narrow peak in graph (c) extends to 3×10^{-6} ergs cm^{-2} s^{-1} but is covered by the inset.

The mean number and duration of pulses for an ensemble of GRBs corresponding to cases (a), (b), and (c) in Figure 2 are 7.9, 19, and 42 and 4.8 s, 1.5 s, and 0.42 s, respectively. Norris et al. (1996) has decomposed 41 bright GRB light curves in order to find a distribution of pulse durations in the range of 0.2–2 s. As shown in the right-hand inset to Figure 2, cloud sizes intermediate to cases (b) and (c) are in accord with the distribution deduced by Norris et al. A distribution of cloud sizes and the addition of background noise in the simulations could improve the comparison.

5. DISCUSSION AND SUMMARY

In the external shock model considered here, STV results from the energy of a blast wave being efficiently extracted by sweeping up matter from the CBM in the form of small clouds (compare the approach of Shaviv & Dar 1995). If the clouds are distributed uniformly around the burst source, then a total cloud mass of

$$M_c \cong 4\Gamma^2 I_c \frac{4\pi}{3} m_p N_{c,\,\min} r^2 \gtrsim 3 \times 10^{-4} \zeta R_{17}^2 \left(\frac{E_{54}}{\Gamma_{300}^2 R_{16}^2}\right) M_\odot \quad (6)$$

is required. Here the minimum cloud column density $N_{c,\,\min}$ is derived for clouds at $10^{16}R_{16}$ cm. In contrast, the minimum mass of the surrounding intercloud medium (ICM) that is required to extract a significant fraction of the blast wave's energy is $E_0/(\Gamma^2 c^2) \approx 6 \times 10^{-6} E_{54}/\Gamma_{300}^2\ M_\odot$. More mass must be in the form of small clouds to ensure that their columns are thick at all values of R, but the total mass is remarkably small in either case. The contrast between the ICM density $n_{\rm ICM}$ and the cloud density n_c that is required to obtain STV is $n_{\rm ICM}/n_c \ll (4f\zeta/\Gamma) \ll 1$. Whether such clouds can be stably confined or whether they must be continuously reformed is unclear.

We consider arguments presented against the external shock model (Fenimore, Ramirez, & Sumner 1998; Fenimore et al. 1996; Sari & Piran 1997; Sumner & Fenimore 1998). The strongest objection is that the overlapping light curves will "wash out" large-amplitude variability. According to equation (2), most clouds produce pulses of duration $\delta t \gtrsim 2ft_{\rm dur}(\Gamma\theta)$. Because most clouds in the Doppler cone are located at $\theta \sim 1/\Gamma$, STV only occurs when $\delta t/t_{\rm dur} \sim f \ll 1$. To obtain a given efficiency, equation (3) shows that $I_c = \zeta/f^2$ clouds with thick columns are required. The number of overlapping clouds in the time element δt is $\approx I_c(\delta t/t_{\rm dur}) \approx fI_c \approx \zeta/f$. This would apparently yield statistical fluctuations on the order of $(f/\zeta)^{1/2}$, which, for $f = 0.01$ and $\zeta = 0.1$, is at the 30% level rather than at the factor of 2 level often seen in GRB light curves.

This argument overlooks the fact that the small fraction of clouds at $\theta \ll 1/\Gamma$ makes a disproportionate contribution to the amplitude and variability of GRB light curves. Only 1% of all clouds in the Doppler beaming cone lie in the range $0 < \theta < 1/(10\Gamma)$, yet the duration of pulses from these clouds is shorter by an order of magnitude than the duration of pulses from clouds at $\theta = 1/\Gamma$. Moreover, the amplitude of the pulses varies according to the factor $\sim\mathcal{D}^{(2+\alpha)}/(\Gamma\theta)$, which represents a factor of ≈ 80 for clouds at $\theta < 1/(10\Gamma)$ when compared with clouds at $\theta \cong 1/\Gamma$. We therefore see that 1% of the clouds produce ≈ 8% of the total fluence in very short duration, very large amplitude pulses. The amplitude enhancements continue to increase proportionally to $1/\theta$ until $\theta \lesssim 1/(2\Gamma^2)$ or until the pulse width becomes limited by other effects. If clouds are found in layers, then the enhanced contribution of on-axis clouds might also overcome the difficulty in producing gaps in GRB light curves (Fenimore et al. 1998).

The efficiency ζ defined in equation (3) represents the most optimistic case where all the blast-wave energy in the region that is energized by the cloud is transformed into radiation. Because the blast wave decelerates strongly in the region of interaction, STV can be produced through Doppler deboosting even if the energized electrons do not lose most of their energy through synchrotron processes (Chiang 1998, 1999). In this case, of course, the efficiency is less than obtained through equation (3).

In summary, we have examined a model in accord with the third scenario described by Fenimore et al. (1996), where STV in GRB light curves is produced by inhomogeneities in the CBM. This breaks the condition of local spherical symmetry, shown by Fenimore et al. to produce light curves inconsistent with observations, but requires the presence of many small clouds with thick columns. As shown here, STV in GRB light curves can be produced by the external shock model under such conditions. Further comparisons of GRB data with model light curves will be necessary, however, to establish whether GRB light curves are tomographic images of the density distributions of the medium surrounding the sources of GRBs.

We thank M. Böttcher, J. Chiang, E. Fenimore, R. Sari, and the anonymous referee for comments and discussions. The work of C. D. D. was supported by the Office of Naval Research and the *CGRO* Guest Investigator Program. The work of K. E. M. was made possible through the Science and Engineering Apprentice Program of George Washington University.

REFERENCES

Baring, M. G., & Harding, A. K. 1997, ApJ, 491, 663
Blandford, R. D., & McKee, C. F. 1976, Phys. Fluids, 19, 1130
Chiang, J. 1998, ApJ, 508, 752
———. 1999, ApJ, submitted (astro-ph/9810238)
Chiang, J., & Dermer, C. D. 1999, ApJ, in press (astro-ph/9803339)
Costa, E., et al. 1997, Nature, 387, 783
Dermer, C. D., Chiang, J., & Böttcher, M. 1999, ApJ, in press (astro-ph/9804174)
Dermer, C. D., Sturner, S. J., & Schlickeiser, R. 1997, ApJS, 109, 103
Djorgovski, S. G., et al. 1997, Nature, 387, 876
Fenimore, E. E., Cooper, C., Ramirez, E., Sumner, M. C., Yoshida, A., & Namiki, M. 1999, ApJ, in press
Fenimore, E. E., Madras, C., & Nayakshin, S. 1996, ApJ, 473, 998
Fenimore, E. E., Ramirez, E., & Sumner, M. C. 1998, in Fourth Huntsville Symp., Gamma-Ray Bursts, ed. C. A. Meegan, R. D. Preece, & T. M. Koshut (New York: AIP), 657
Feroci, M., et al. 1998, A&A, 323, L29
Kulkarni, S., et al. 1998, Nature, 393, 35
Mészáros, P., Laguna, P., & Rees, M. J. 1993, ApJ, 415, 181
Mészáros, P., & Rees, M. J. 1993, ApJ, 405, 278
Norris, J. P., et al. 1996, ApJ, 459, 393
Piro, L., et al. 1998, A&A, 331, L41
Rees, M. J., & Mészáros, P. 1992, MNRAS, 258, 41P
Sari, R., & Piran, T. 1997, ApJ, 485, 270
Shaviv, N., & Dar, A. 1995, MNRAS, 277, 287
Sumner, M. C., & Fenimore, E. E. 1998, in Fourth Huntsville Symp., Gamma-Ray Bursts, ed. C. A. Meegan, R. D. Preece, & T. M. Koshut (New York: AIP), 765
van Paradijs, J., et al. 1997, Nature, 386, 686
Vietri, M. 1997, ApJ, 478, L9
Waxman, E. 1997, ApJ, 485, L5
Wijers, R. A. M. J., Rees, M. J., & Mészáros, P. 1997, MNRAS, 288, L51